

Empirical oscillating potentials for alloys from ab-initio fits

Marek Mihalkovič,^{1,2} C. L. Henley,¹ M. Widom,³ and P. Ganesh^{3,4}

¹Laboratory of Atomic and Solid State Physics, Cornell University, Ithaca, NY, 14853-2501

²Permanent address, Institute of Physics, Slovak Academy of Sciences, 84228 Bratislava, Slovakia.

³Dept. of Physics, Carnegie-Mellon University, Pittsburgh, PA, 15213

⁴Current address: Carnegie Institution of Washington, GL, 5251 Broad Branch Road, NW, Washington, DC, 20015

By fitting to a database of ab-initio forces and energies, we can extract pair potentials for alloys, with a simple six-parameter analytic form including Friedel oscillations, which give a remarkably faithful account of many complex intermetallic compounds. As examples we show results for (crystal or quasicrystal) structure prediction and phonon spectrum for three systems: Fe–B, Al–Mg–Zn, and Al–Cu–Fe.

PACS numbers: 02.70.Ns, 61.50.Lt, 63.20.Dj, 64.70.Kb, 61.44.Br

Several kinds of problem in materials modeling can be addressed only by classical interatomic potentials. Consider complex alloy crystal structures: it is impossible to use diffraction-data refined structures straightforwardly, for they almost always contain sites with mixed or fractional occupancies. These must be resolved properly to evaluate physical properties, which can be unfeasible with current fast ab-initio codes using density functional theory, such as VASP [1]. Only moderate resources are needed for *single* evaluations of the total energy, but repeated evaluations are prohibitive for unit cells having up to 10^3 atoms per cell; even if just 1–5% of the sites are uncertain, one must examine a vast number of variant structures to assign the occupancies optimally. In any case, classical potentials are required when the structure has no tractable unit cell (quasicrystals or amorphous metals); they also facilitate dynamic or thermodynamic simulations (phonon spectra and phase transformations in complex alloys).

A common modern approach to modelling atomic interactions classically is the “embedded-atom method” (EAM) [2] as well as “modified EAM” [3], in which the full Hamiltonian contains the usual pair term $V_{ij}(R)$, but also an implicitly many-atom term $U(\rho)$, where ρ is a sum of contributions from nearby atoms. Accurate EAM potentials are straightforward to extract for monatomic systems [4] but demand patience and skill to obtain even for binary systems [5, 6]; obviously, dimensionality of parameter space becomes critical for multi-component systems.

In this paper we report on an alternative approach [7] fitting only pair interactions but incorporating Friedel oscillations, optimized (typically) for a particular composition range. The oscillating analytical form is natural only for simple metals (Al, Mg,...) yet (see below) it works surprisingly well even when angular or many-body interactions are important. We will first describe the form of the potential and our methods for fitting it, then demonstrate its capabilities through case studies in three alloy systems: Fe–B, Al–Mg–Zn, and Al–Cu–Fe; finally, we will summarize other systems where this method has been applied and discuss its limitations.

Method: potential, database, and fitting — Our “empirical

oscillating pair potentials” (EOP) have the form

$$V(r) = \frac{C_1}{r^{\eta_1}} + \frac{C_2}{r^{\eta_2}} \cos(k_* r + \phi_*) \quad (1)$$

All six parameters, including k_* , are taken as independent in the fit for each pair of elements. Eq. (1) was inspired by effective potentials (e.g. [8] and [9]) used in previous work on structurally complex metals, e.g. quasicrystals [7, 10, 11]. In such systems, energy differences between competing structures are often controlled by second- and third-neighbor wells due to Friedel oscillations, which are a consequence (mathematically) of Fourier transforming the Fermi surface, or (physically) are equivalent to the Hume-Rothery stabilization by enhancing the strength of structure factors that hybridize states across the Fermi surface. [12] In the framework of Ref. 12 (Sec. 6.6), the short-range repulsion is captured by the first term of (1); the medium-range potential (first-neighbor well) as well as the long-range oscillatory tail are captured by the second term, their relative weights being adjusted by the η_i parameters. Note that empirically fitted potentials account for some of the many-body contributions within their pair terms, which works better practically than truncating a systematic expansion (e.g. GPT [13]) after the pair terms.

The parameters in (1) are fitted to an ab-initio dataset (we always used the VASP code [1]) combining both relaxed $T = 0$ structures and molecular dynamics (MD) simulations at high T (usually the same structures, below the melting point.) Structures are selected for the database within, or bracketing, the composition range of interest; when possible, a mix of simple and complex structures is used. A key criterion in choosing structures is to ensure an adequate number of contacts of each kind (in particular, nearest-neighbor contacts between the least abundant species). Also, all structures in the database should have similar atom densities [14]. In particular, our high- T MD samples were constrained to have the *same* density as at $T = 0$, rather than the physical zero-pressure values. In MD simulations of the simpler structures, a supercell is always used with dimensions comparable to the potential cutoff radius, which (in this paper) is always 12\AA .

We define each structure’s energy as a difference relative to a coexisting mixture (with the same total composition) of ref-

system	B-Fe	Al-Mg-Zn	Al-Cu-Fe
ref.	Fe, BFe ₂	Al, Mg, Zn	Al ₇ Cu ₂ Fe Al ₂ Cu, Al ₂ Fe
data-base	BFe ₂ [Al ₂ Cu] BFe ₃ [CFe ₃] BFe ₃ [Ni ₃ P] B ₆ Fe ₂₃ [C ₆ Cr ₂₃] B ₃ Fe ₄ [B ₃ Ni ₄] B ₁ Fe ₁ [BCr] <i>a</i> -Fe ₈₀ B ₂₀	MgZn ₂ [Laves] <i>T</i> (Al ₉₆ Mg ₆₄) [<i>T</i> (AlMgZn)] <i>T</i> (Zn ₉₆ Mg ₆₄) [<i>T</i> (AlMgZn)] Al ₁₂ Mg ₁₇ AlMg ₄ Zn ₁₁ <i>β'</i> -Al ₃ Mg ₂	Al ₆ Fe Al ₅ Fe ₂ [Al ₂₃ CuFe ₄] Al ₂ Cu Al ₇ Cu ₂ Fe Al ₂₃ CuFe ₄ Al ₇₂ Cu ₄ Fe ₂₄ [Al ₃ Fe] “1/1-expe” “1/1-6D”
T_{MD}	1500	450 (Al-Mg); 1000 (Mg-Zn)	500 (“1/1-6D”); 1200 (“1/1-6D”); 1000 (Al ₇ Cu ₂ Fe)

TABLE I: Compounds used in each database used to fit potentials. Energies are expressed as difference from the tie-line or tie-plane defined by the simple reference structures listed; these structures are also included in the database. In brackets are the conventional names for crystal structure type. The temperature (in K) used for molecular-dynamics samples is T_{MD} (where compositions are given, those are the only $T > 0$ inputs)

reference phases, chosen to bracket all database compositions. Every structure is used for both forces (from MD at high T) and energy differences [15] (high- T MD, as well as relaxed at $T = 0$). For the high- T portion, we took one snapshot of each structure at the end of a short ab-initio MD run. Typically $\sim 10^3$ force components entered the fit, along with ~ 50 energy differences (more for Al-Mg-Zn, fewer for Fe-B), and the forces are $\sim 2\text{--}4$ eV/Å while the energy differences are $\sim 0.2\text{--}0.4$ eV/atom; the fit residuals are $\sim 5\%$ and $\sim 1\%$ respectively.

Our least-squares fit minimizes (by the Levenberg-Marquardt algorithm) $\chi^2 \equiv \sum \Delta E_i^2 / \sigma_E^2 + \sum |\Delta \mathbf{F}_j|^2 / \sigma_F^2$, where $\{\Delta E_i\}$ and $\{\Delta \mathbf{F}_j\}$ are the energy and force residuals; we found a weighting ratio $\sigma_E / \sigma_F \sim 10^{-3} \text{Å}$ was optimal so that neither energies nor forces dominate the fit. There is some risk of converging to a false minimum (or not converging at all, from an unreasonable initial guess). Thus, it is important to repeat the fit from several starting guesses. For this we used, e.g., potentials first fitted to pure elements or binary systems, and also used a library of parameter sets previously fitted for some different alloy system. The fitted parameters in (1 for each of our examples are available as supplementary information [16]; similar potentials were plotted in Refs. [17] (for Al-Mg) and [18] (for Sc-Zn)

Example 1: B-Fe. — Amorphous B-Fe is the simplest member of a family of technologically important metallic glasses. Our B-Fe database (Table I) included several crystals plus an “amorphous” sample with 100 atoms in an approximately cubic box. The ab-initio data were calculated with a spin polarization so as to include magnetic contributions to the forces/energies. [19] For comparison, we also fitted the database to Lennard-Jones (LJ) potentials which lack oscilla-

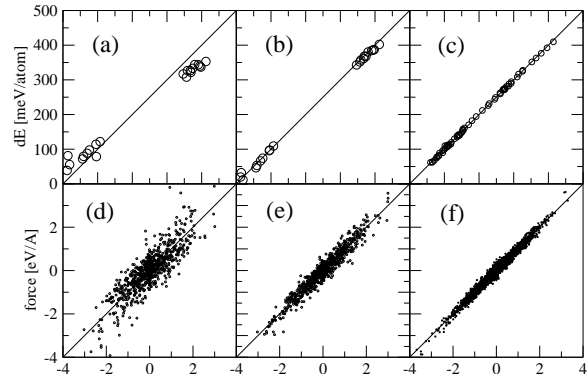


FIG. 1: Scatter plot of pair potential result (vertical axis) versus ab-initio data (horizontal axis) for energy differences ΔE_i (top panels) and forces \mathbf{F}_j (bottom panels). The potentials are: (a,d) Lennard-Jones fit to B-Fe, (b,e) EOP fit [Eq. (1)] to B-Fe, and (c,f) EOP fit to Al-Mg-Zn.

tions (starting this fit from the Kob-Anderson potentials [20]).

We employed a modified tempering scheme [21] with replica exchange. That means two simulations were carried out for 100-atom samples of Fe₈₀B₂₀ at $T=1500\text{K}$, one using the ab-initio energy as its Hamiltonian and the other using EOP. At intervals a Monte Carlo (MC) attempt is made to swap the two samples. These swaps accelerate the configuration sampling. The acceptance probability (we had $\sim 70\%$ for Fe-B) is a stringent test of how well the pair-potential Hamiltonian mimics the ab-initio one.

The superiority of the EOP form over LJ is evident from the excellent diagnostic of scatter plots in Fig. 1. As another diagnostic, Fig. 2, shows the radial distribution functions found in an MD run at $T = 1500\text{K}$, using the ab-initio energies as well as both kinds of pair potential; the EOP form faithfully reproduced all features of the ab-initio data.

Example 2: Al-Mg-Zn — In this example, EOP potentials resolve site occupancies and the phase diagram of low-temperature modifications of the well-known cubic “Bergman” compound T(AlMgZn) [22, 23] (X-rays can hardly distinguish Al from Mg ions, as they differ by only one electron.) Our database (Table I) spanned the entire range of ternary compositions. (Al-Mg-Zn was previously modeled using pseudo-binary pair potentials, [11].)

The EOP potentials were then used in a lattice-gas type MC annealing (using sites from diffraction [22, 23]) for each of 91 compositions, with 52–64 Mg atoms and 24–72 Al atoms per cell (thus spanning the full Al-Zn range, and $\pm 5\%$ in Mg concentration). For 21 selected candidate structures, we subsequently did a full ab-initio calculation. Four of these structures (Table II) were stable at $T = 0$. The first of these is the standard structure [22] (but with empty-centered icosahedral clusters); the second one differs by converting the Mg

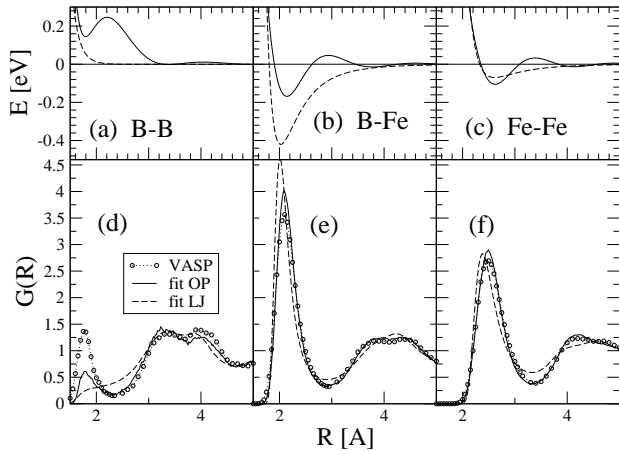


FIG. 2: a,b,c: B-Fe pair potentials (c,d,e): Corresponding radial distribution functions at 1500K, using ab-initio energies (dotted), empirical oscillating pair-potentials (solid), or fitted Lennard-Jones potentials (dashed).

composition	Al(2)	Mg(3)	Zn(1)	sp. gr.	ΔE_{VASP}	ΔE_{pair}
Al ₂₄ Mg ₆₄ Zn ₇₂	1	0	0	$Im\bar{3}$	-122.1	-117.3
Al ₃₆ Mg ₅₂ Zn ₇₂	1	1	0	$Im\bar{3}$	-114.1	-109.0
Al ₄₈ Mg ₆₄ Zn ₄₈	2/3	0	1/3	$Immm$	-92.8	-92.2
Al ₆₆ Mg ₅₈ Zn ₃₆	1/4	1/2	0	$R\bar{3}$	-77.9	-76.1

TABLE II: The four stable low-temperature modifications of the Bergman phase $T(\text{AlMgZn})$: the occupation is given (as a fraction) of Zn on Al(2) site, Al on Mg(3) site and Al on Zn(1) site, followed by the space group. Our site labels (Al/Mg/Zn) correspond to F/G/B in Ref. [23]. $\Delta E_{\text{VASP,pair}}$ are the total energy (per atom, in eV) of each structure minus the reference (tie-plane) energy.

atoms with coordination 14 (the smallest for Mg) to Al atoms. We applied the same method to the recently solved $\beta'(\text{AlMg})$ structure [17], a low- T variant of Samson’s very large-cell $\beta(\text{AlMg})$ [24]; at $T = 0$ $\beta'(\text{AlMg})$ is essentially a line compound.

Example 3: Al-Cu-Fe — The structures of the best thermodynamically stable icosahedral quasicrystals, e.g. $i\text{-Al-Mn-Pd}$ and $i\text{-Al-Cu-Fe}$, are poorly known despite excellent long-range order and 20 years of study. This extends to $\alpha\text{-AlCuFe}$, the so-called 1/1 cubic approximant to the quasicrystal (it is related to $i\text{-AlCuFe}$ in the same way that $T(\text{AlMgZn})$ [see above] is related to $i\text{-AlMgZn}$.)

Diffraction-based modeling, by itself, rarely resolves all the important structural details; this is apparent even in the $\alpha\text{-AlCuFe}$ crystal, for which the “solved” structure [25] contains mixed-occupancy Al-Cu and Al-Fe sites; that uncertainty, is a substantial obstacle to realistic modelling of quasicrystal properties: the ab-initio energy of such a model is, we expect, unstable by ~ 100 meV/atom with respect to competing phases [26]; the idealized and improved model [27] is, we found, unstable by 51 meV/atom. The root of the difficulty is that strong local correlations have not been accounted for, due to the averaging inherent in using Bragg peak intensities.

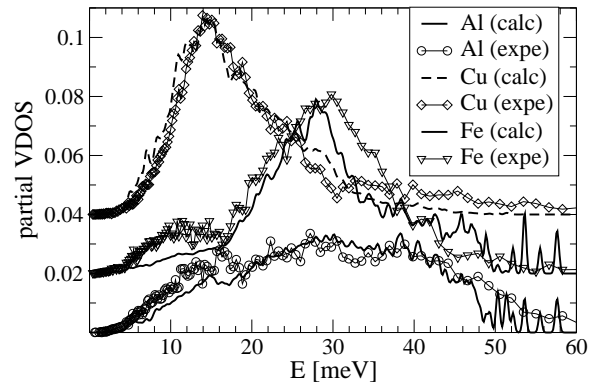


FIG. 3: Partial phonon densities of states for Al, Cu and Fe: “calc” calculated (“calc”) using EOP potentials, experimental (“exp”) data after Ref. [31].

We set up a robust database with 15312 force and 120 energy datapoints (see Table I). The fit converged to 0.2 eV/Å r.m.s. for forces and 8 meV/atom for energies. To refine the atomic structure of $\alpha(\text{AlCuFe})$, we took candidate sites from two diffraction-based models, either from $\alpha(\text{AlCuFeSi})$ [25], or 1/1-AlCuRu [28], and performed a lattice-gas Monte Carlo annealing using EOP potentials. The best configurations were then annealed by MD (still using EOP) at moderately high temperatures ($T = 1000\text{K}$) and finally quenched. When their energies were recalculated ab-initio, the best example was still unstable, but only by the relatively small energy 35 meV/atom. The lowest energy structure obtained as described above was then used for phonon DOS calculation by diagonalizing the dynamical matrix. The agreement between calculated and experimental DOS (Fig. 3) is encouraging.

EOP potentials were also applied to predict the atomic structure of the quasicrystal $i\text{-Al}_{67.5}\text{Cu}_{25}\text{Fe}_{12.5}$, by similar lattice-gas approach using (a periodic approximant of) a “quasilattice” of candidate sites. [29] The resulting structures were well-described by the formalism of a cut through a six-dimensional hyper-structure, but the hyper-atom occupancies differ in detail from the well-known Katz-Gratias model [30]. The ab-initio energy after relaxation was unstable (with respect to the competing phases [26]) by 45 meV/atom. The computed vibrational DOS agrees with neutron results [31].

Conclusion. — We have shown that empirical oscillating potentials with the simple analytic form (1) mimic the atomic interactions of many metallic systems with sufficient accuracy to stand in for ab-initio energies when those would be computationally prohibitive, e.g. to resolve mixed or partially occupied sites in diffraction refinements of complex structures, to measure thermodynamic expectations, or to compute phonon spectra.

The easily obtained EOP potentials may serve as a starting point for the (tedious) construction of (more elaborate) EAM versions of the potentials. Furthermore, EOP potentials can accelerate ab-initio calculations, to identify uncompetitive al-

ternatives to be ignored (as in our Al-Zn-Mg example) or to carry out all but the final iterations of a relaxation. EOP potentials appear to be fitted more robustly than EAM potentials for 4-component systems; we fitted B-C-Fe-Mo which enables for the first time MD simulations of technologically relevant metallic glasses (to probe the glass transition, two-level systems, etc.). It should be noted, however, that *any* pair potential will fail in structures where the electron density has large variations in space (e.g. vacancies, edge dislocations, or surfaces).

Rather than emphasize the easy cases (alloys rich in simple metals, e.g. AlMgZn, Mg-X, but also Zn-Y), we presented two difficult examples (B-Fe and Al-Cu-Fe), which are borderline for pair potentials, due to covalent bonding of nearest neighbor transition metals. In the many cases where bond directionality is even more important, EOP potentials cannot be used.

Our method had mixed success for pure elements: Al-Al potentials show an excellent fit to the ab-initio data, with Mg-Mg even better. But with pure Zn, pair potentials never reproduced the ab-initio phonon vibrational DOS; and the EOP approach fails for pure Ga.

EOP potentials show promise for many other alloy systems. They allowed extraction of long-wavelength phonons from molecular dynamics simulations [33] in liquid Bi-Li system. Outstandingly accurate EOP were fitted for the system Mg-T (T=Pd or Ag) in the Mg-rich limit; for T=Ag, the Ag-Ag potential exhibits strong oscillations to large r that could only be fitted after the cutoff was extended to to 14Å [32]. These systems include various complex phases based on icosahedral “Mackay” clusters (Mg₄₂X₁₂). EOP potentials have predicted – correctly – which Mg sites get substituted by Pd as the composition is varied [32] in the phases γ (Mg_{0.8}Pd_{0.2}) and δ (Mg_{0.8}Pd_{0.2}) [both “1/1 approximants”, similar in structure to α -AlMnSi].

We thank R. G. Hennig and F. Gähler for comments. We supported by DOE Grant DE-FG02-89ER-45405 (MM, CLH), the DARPA Structural Amorphous Metals Program under ONR Grant N00014-06-1-0492 (MW, MM, PG), and Slovak funding VEGA 2/0157/08 and APVV-0413-06 (MM).

pair	C_1	η_1	C_2	η_2	k_*	φ_*
B–B	11.69	5.184	8.338	5.149	3.950	2.617
B–Fe	2372.51	17.232	-6.043	4.441	3.994	3.637
Fe–Fe	1.443×10^5	18.556	4.939	3.934	4.074	4.651
Al–Al	2669	10.37	-4.93	4.41	3.88	-4.38
Al–Mg	4296	10.61	-39.4	6.21	3.33	-4.02
Mg–Mg	14.59	4.79	183.3	6.49	2.19	-4.53
Al–Zn	949	9.36	-2.52	3.36	3.33	-2.16
Mg–Zn	282	8.26	-31.7	5.58	2.82	-2.26
Zn–Zn	706	9.33	-6.01	4.33	3.69	-3.48
Al–Al	4.431×10^5	15.990	-0.577	3.410	4.680	5.372
Al–Fe	1.842×10^5	18.713	7.884	3.609	3.079	1.730
Al–Cu	3096.1	12.079	-1.457	3.261	3.687	2.978
Fe–Fe	125.26	8.081	1.115	2.504	4.477	1.708
Fe–Cu	23.13	5.856	0.323	1.520	3.086	1.947
Cu–Cu	11304	12.631	-2.124	3.301	2.830	0.159

TABLE III: Parameters for B–Fe, Al–Mg–Zn and Al–Cu–Fe potentials [Eq. (1)], with r in units of Å and $V(r)$ in eV.

- [1] (a) G. Kresse and J. Hafner, Phys. Rev. B, 47, R558 (1993); (b) G. Kresse and J. Furthmuller, Phys. Rev. B 54, 11169 (1996).
- [2] M. S. Daw and M. I Baskes, Phys. Rev. B 29, 6443 (1984).
- [3] M. I. Baskes, Phys. Rev. Lett. 59, 2666 (1987); see e.g. B. Jelinek *et al*, Phys. Rev. B 75, 054106 (2007).
- [4] S. M. Foiles, M. I. Baskes, and M. S. Daw, Phys. Rev. B 33, 7983 (1986); PRB 33, 7983 (1986); J. E. Jaffe, R. J. Kurtz and M. Gutowski, Comput. Mater. Sci. 18, 199 (2000). T. J. Lenosky *et al*, Modelling Simul. Mater. Sci. Eng. 8, 825 (2000).
- [5] J. D. Althoff *et al*, Comput. Mater. Sci. 10, 411-15 (1998); R. Zope and Y. Mishin, Phys. Rev. B 68, 024102 (2003)
- [6] P. Brommer and F. Gähler, Philos. Mag. 86, 753 (2006).
- [7] M. Mihalkovič, Acta Physica Slovaca, to be published.
- [8] J. Hafner, *From Hamiltonians to Phase Transitions* (Springer, Heidelberg, 1987).
- [9] J. A. Moriarty and M. Widom, Phys. Rev. B 56, 7905 (1997).
- [10] (a). M. Mihalkovič *et al* Phys. Rev. B 53, 9021-45 (1996); (b) M. Mihalkovič *et al*, Phys. Rev. B 65, 104205 (2002).
- [11] M. Krajčí and J. Hafner, Phys. Rev. B 46, 10669 (1992).
- [12] D. Pettifor, *Bonding and Structure of Molecules and Solids* (Oxford Univ. Press, Cambridge, 1995).
- [13] (a) J. A. Moriarty, Phys. Rev. B 16, 2537 (1977); (b). Phys. Rev. B 26, 1754 (1982).
- [14] For a successful fit, the database must be limited to a relatively narrow range of (electron) densities, so the Fermi wavevector [hence k_* in Eq. (1)] has a consistent value.
- [15] Fits from forces alone were insufficiently constrained; including energy differences, even with low weight, improved the fit.
- [16] Tables of parameters in Eq. (1) for Fe-B, Al-Zn-Mg, and Al-Cu-Fe will be placed in the APS Depository (and on arxiv...).
- [17] M. Feuerbacher *et al*, Z. Kristallogr. 222, 259 (2007)
- [18] M. de Boissieu *et al*, Nature Mater. 6, 977-984 (2007).
- [19] P. Ganesh and M. Widom, Phys. Rev. B (2008, in press)
- [20] W. Kob and W. C. Andersen, Phys. Rev. E 48, 4364 (1993).
- [21] E. Lyman, F. M. Ytreberg, and D. M. Zuckerman, Phys. Rev. Lett. 96, 028105 (2005).
- [22] G. Bergman, J. L. T. Waugh, and L. Pauling, Acta Crystallogr. 10, 254 (1957).
- [23] U. Mizutani *et al*, Phil. Mag. Lett. 76, 349 (1997).
- [24] S. Samson, Acta Crystogr. 19, 401 (1965).
- [25] F. Puyraimond *et al* Acta Crystallogr. A 58, 391 (2002).
- [26] Competing Al-Cu-Fe phases: m -Al₃Fe, its ternary variant Al₇₂Cu₄Fe₂₄ and monoclinic AlCu.
- [27] E. Cockayne *et al* J. Non-Cryst. Solids 153&154, 140 (1993); E. S. Zijlstra *et al*, Phys. Rev. B 69, 094206 (2004).
- [28] K. Sugiyama *et al*, J Alloy Compounds 299, 169 (2000)
- [29] M. Mihalkovič and C. L. Henley, unpublished.
- [30] M. Quiquandon and D. Gratias, Phys. Rev. B 74, 214205 (2006), and references therein.
- [31] (a). P. P. Parshin *et al.*, Fiz. Tverd. Tela 46, 510 (2004) [Phys. Solid State 46, 526 (2004)]; (b) P. P. Parshin, M. G. Zemlyanov and R. A. Brand, JETP 101, 676 (2005).

- [32] M. Mihalkovič and G. Kreiner, unpublished.
- [33] J.-F. Wax, M. Johnson, M. Mihalkovič *et al*, in preparation